### Title

Glycocalyx transduces membrane leak in brain tumor cells exposed to sharp magnetic pulsing.




### Journal

Biophysical Journal, 122(22)



### Authors

Johns, Scott

Gupta, Purva

Lee, Yi-Hung

et al.



### Publication Date

2023-11-21

### DOI

10.1016/j.bpj.2023.10.020

Peer reviewed

Biophysical Journal
Article

Biophysical Society

# Glycocalyx transduces membrane leak in brain tumor cells exposed to sharp magnetic pulsing

Scott C. Johns,[1,2] Purva Gupta,[1,3] Yi-Hung Lee,[5] James Friend,[6] and Mark M. Fuster[1,2,3,4,*]
[1]VA San Diego Healthcare System, San Diego, California; [2]Veterans Medical Research Foundation, San Diego, California; [3]Department of Medicine, Division of Pulmonary & Critical Care, University of California San Diego, La Jolla, California; [4]Glycobiology Research and Training Center, University of California San Diego, La Jolla, California; [5]Department of Bioengineering, University of California San Diego, La Jolla, California; and [6]Department of Mechanical and Aerospace Engineering, University of California San Diego, La Jolla, California

ABSTRACT Mechanisms by which electric (E) or magnetic (B) fields might be harnessed to affect tumor cell behavior remain poorly defined, presenting a barrier to translation. We hypothesized in early studies that the glycocalyx of lung cancer cells might play a role in mediating plasma membrane leak by low-frequency pulsed magnetic fields (Lf-PMF) generated on a low-energy solenoid platform. In testing glioblastoma and neuroblastoma cells known to overexpress glycoproteins rich in modifications by the anionic glycan sialic acid (Sia), exposure of brain tumor cells on the same platform to a pulse train that included a 5 min 50Hz Lf-PMF (dB/dt $\sim$ 2 T/s at 10 ms pulse widths) induced a very modest but significant protease leak above that of control nonexposed cells (with modest but significant reductions in long-term tumor cell viability after the 5 min exposure). Using a markedly higher dB/dt system (80 T/s pulses, 70 $\mu$s pulse-width at 5.9 cm from a MagVenture coil source) induced markedly greater leak by the same cells, and eliminating Sia by treating cells with AUS sialidase immediately preexposure abrogated the effect entirely in SH-SY5Y neuroblastoma cells, and partially in T98G glioblastoma cells. The system demonstrated significant leak (including inward leak of propidium iodide), with reduced leak at lower dB/dt in a variety of tumor cells. The ability to abrogate Lf-PMF protease leak by pretreatment with sialidase in SH-SY5Y brain tumor cells or with heparin lyase in A549 lung tumor cells indicated the importance of heavy Sia or heparan sulfate glycosaminoglycan glycocalyx modifications as dominant glycan species mediating Lf-PMF membrane leak in respective tumor cells. This "first-physical" Lf-PMF tumor glycocalyx event, with downstream cell stress, may represent a critical and "tunable" transduction mechanism that depends on characteristic anionic glycans overexpressed by distinct malignant tumors.

SIGNIFICANCE Malignant tumors characteristically overexpress glycans that carry anionic charge at physiological pH in the tumor cell glycocalyx, a layer or "canopy" of complex carbohydrates that coats the cell surface with protein or lipid core attachments to the tumor plasma membrane. Distinct from that of normal cells, the unique glycan-dense tumor glycocalyx may be susceptible to electromotive forces generated by Lf-PMFs over continuous tumor cell surfaces, with tumor plasma membrane leak (and downstream cell stress) as a result of membrane shear forces or molecular torque imposed by EMF pulsed movement of the overlying glycocalyx. This mechanistic understanding represents an opportunity for selective targeting of tumor cells in novel clinical platforms.

## INTRODUCTION

The use of oscillating magnetic fields to alter cancer cell growth has been described in biophysics, but the field strengths, frequencies, and/or characteristics to consistently induce cancer cell death or tumor regression in biological models remain a mystery (1–4). This is more generally appreciated in light of a variety of biological effects that may result from very low to high intensities and/or frequencies of experimental and environmental magnetic fields (summarized in (5)). We recently discovered that "pulsed" magnetic fields induce electromotive forces (EMFs) that engage with charged complex carbohydrate (glycan) molecules that occupy the "glycocalyx" of cancer cell membranes (6). This results in membrane leak and imposes a modest inhibition in tumor cell viability in preliminary studies. Unlike cancer radiotherapy that targets high-energy ionizing radiation to S-phase DNA of rapidly dividing tumor cells, we hypothesize that low-frequency narrow pulse-width (i.e., "sharp")

*Submitted February 24, 2023, and accepted for publication October 19, 2023.*

*Correspondence: mfuster@ucsd.edu

Editor: Guy Genin.
https://doi.org/10.1016/j.bpj.2023.10.020



magnetic fields, characterized by a high dB/dt pulse quality, can be used to selectively couple with this unique cancer cell surface glycan layer (6–8). Under unique spatial and temporal conditions, this may disrupt tumor membrane integrity. Low-frequency oscillating magnetic fields have been shown to inhibit tumor growth in mice (3,4,9), although mechanisms, including unique effects of the pulsed-field magnitude and width (or pulse "sharpness" defined by dB/dt) on tumor membrane leak as well as any transducing capability of glycocalyx in this process have not been described. Thus, while efficacy in altering neoplastic cell growth in some in vitro and in vivo models has been shown (3,4,10,11), knowledge on biophysical mechanism(s), cancer cell-specific effects, and the connection between cellular physiology and in vivo applications remains undefined. Nevertheless, the majority of studies show an inhibitory effect on tumor cell growth. In some cases, very low frequencies are used (3,10,12,13), and we found it intriguing to consider how the tumor cell surface, with any given "sharp" magnetic pulse (i.e., independent of frequency), may transduce a corresponding physical effect, such as membrane leak, with downstream cell stress that may follow.

We sought to understand how magnetic pulsing conditions on distinct sets of neoplastic cell monolayers (and distinct glycocalyx compositions) may be susceptible to membrane-altering effects of low-frequency pulsed magnetic fields (Lf-PMFs) with well-controlled pulse intensities. Conceptually, a heavily charged glycocalyx expressed over a continuous surface layer on multiple adjacent tumor cells may ultimately be susceptible to a conductive EMF induced by a pulsed magnetic field perpendicular to the cell plane with magnitude proportional to dB/dt by Faraday's law of induction (14), and where the magnitude of the EMF may be augmented if it bounds a larger area (A) of continuous glycocalyx over which dB/dt is fluxed (where EMF $\sim$ A(dB/dt)). This may alter membrane integrity with an effect sufficient to leak proteases, as measured by commercial cytotoxicity assays under defined Lf-PMF conditions in cultured tumor cells (6). We aimed to more generally consider whether neoplasms may overexpress distinct families of charged glycans typically found on the tumor cell surface, including glycoprotein termini heavily modified by sialic acid (Sia) in addition to anionic glycosaminoglycans, which include sulfated species such as heparan sulfate (HS), chondroitin sulfate (CS), or non-sulfated hyaluronan (HA). With a specific focus on Sia, that monosaccharide contains an anionic negatively charged oxygen atom (at physiological pH), and decorates the termini of polyantennary O-linked and N-linked glycans overexpressed on tumor glycoproteins (15–20). While certain tumors overexpress distinct proteoglycans into the tumor glycocalyx, others overexpress heavy Sia modifications on glycoproteins or polysialic acid (polySia) chains extended on glycan termini decorating unique tumor core proteins (18,21–23).

A unique class of neoplastic cells that often overexpress Sia in the glycocalyx includes that of brain neoplasms such as glioblastoma and neuroblastoma (18,24). The latter often express polySia (e.g., as in the model SH-SY5Y cell line), which may project high levels of negative charge into the glycocalyx (23), a property contributing to cell-cell repulsion which facilitates tumor tissue invasion and metastatic progression (16,24). Demonstrating how Lf-PMF-induced membrane disruption may be sensitive to destroying or removing a specific anionic glycan in the glycocalyx of specific tumor cells may be helpful in defining the importance of that specific glycan in mediating the EMF-driven leak in that unique tumor type. We focused on Sia-overexpressing brain tumor lines as models to study susceptibility and mechanistic dependence of tumor cellular protease leak patterns in response to controlled Lf-PMFs. This included consideration as to whether sialidase-mediated clearance of Sia on tumor cells might render tumor cells less sensitive to Lf-PMF alterations in membrane integrity. We also examined a lung cancer cell line that is also susceptible to high dB/dt Lf-PMFs, albeit with unique sensitivity to the presence/absence of distinct charged glycans (HS) that may at least functionally "dominate" the glycocalyx of such cells. It should be noted that brain tumors (especially high-grade gliomas and neuroblastomas) often overexpress Sia heavily on the glycocalyx (18,24–26), which correlates with their aggressiveness. This includes well-documented overexpression in glioblastoma lines T98G and A172 (27,28) and the neuroblastoma line SH-SY5Y (23). So, as a proof-of-concept herein, we focused on magnetosensitivity of brain tumors, and Sia as a key brain malignancy anionic glycan overexpressed on the brain tumor glycocalyx.

Our findings suggest the importance of what are likely EMF-mediated forces by Lf-PMFs on tumor cell glycocalyces composed of a considerable presence of Sia in representative brain tumor cell lines, and where transduction of such forces via attachment to membrane-bound core proteins may induce membrane stress and leak. On the other hand, distinct glycans appear to mediate the effects in distinct tumors; but to test principles, a relatively high-intensity dB/dt could practically be applied using a transcranial magnetic stimulation type system to drive uniquely configured coils to accommodate cultured cells in perpendicularly fluxing fields across the cells. To our knowledge, this system has not been applied to tumor cell systems, and the role of the malignant cell glycocalyx has not been examined as a mechanical transducer of dB/dt-driven EMFs in distinct tumor types with distinct anionic glycan compositions. The insights may facilitate rational translational considerations from the mechanistic principles suggested herein.

## MATERIALS AND METHODS

### Cell culture and field-exposure preparations

The commercial human glioblastoma cell lines T98G and A172 were grown in cell culture at 37°C in EMEM and DMEM minimal essential culture media, respectively, supplemented with 10% fetal bovine serum (FBS); and the human neuroblastoma cell line SH-SY5Y (short-name denoted SHSY herein) was grown in EMEM containing 10% FBS. The human lung adenocarcinoma

cell line A549 was grown in F-12K medium supplemented with 10% FBS. Cells were also supplemented with 1% PenStrep (Gibco; Waltham, MA) and subcultured once they reached 80% confluency using a 0.5% trypsin 0.2% EDTA solution to lift cells; and plated into either 96-well (96W) or 12-well (12W) format, depending on the assay being used. For most studies involving magnetic field exposures, cells were seeded at $1.0 \times 10^4$ cells per well in 96W cell culture plates, and allowed to grow for 48 h before magnetic field exposure (when cells were typically approximately 70–90% confluent). As a typical primary cell type (immune monocyte) that might be found in the tumor microenvironment, cultured primary bone marrow-derived dendritic cells were isolated as in (29), and seeded into 96W plates at day 7 of primary cell growth at $5.0 \times 10^4$ cells per well, and settled over 3 days before magnetic field exposure. For a subset of studies (employing a low-intensity solenoid pulsed magnet field platform), T98G tumor cells were seeded at $2.0 \times 10^4$/well in 96W plates, while settling overnight before magnetic field exposure, with a similar 70–90% confluence achieved before field exposure. For cultured cell-growth studies after field exposure, cells seeded at $1.0 \times 10^5$ in 12W plates were exposed to low-intensity magnetic fields on a solenoid platform followed by daily cell counts for 3 days growth postexposure.

## Magnetic field platforms and exposures

For most experiments, a Lf-PMF system was used. The source coil was connected to a MagVenture (Alpharetta, GA) unit used for transcranial magnetic stimulation (30), with application using a Cool 40 Rat-Coil (31) trough-shaped platform generating dB/dt in a 2D ring-shaped spherical-field cross section from the trough base (coil center). The trough was laterally oriented with a 96W plate inserted in the field so that fluxing B-lines would run perpendicular to (and across) the plated monolayer tumor cells on 96W plate bottom surfaces (illustrated in Fig. S1, which also includes schematic descriptions of the pulse sequences). Magnetic pulses were delivered to plated cells at a relatively high ratio of amplitude to pulse width for a 5 min exposure period at room temperature, and consisted of oscillating fields with a duty-cycle pulse width of 70 $\mu$s using 15-Hz pulse trains, with dB/dt $\sim$ 80 T/s for 96W plated cells centered and fluxed over a high-intensity zone positioned 5.9 cm from the magnetic coil center ("near" zone) versus $\sim$1.8 T/s at a more distal zone ("far" zone) of exposure positioned 10.5 cm from the coil center. These values correspond to the running unit output set at 10% maximum (relative to maximum dB/dt by the coil source) for all 5 min runs to ensure constant output conditions with optimal standardized coil cooling for the above pulse-train settings. In a subset of experiments, to reference an original prototype platform, some plated tumor monolayers were exposed to a simple low-intensity oscillating B-field solenoid (used as in (6)) placed immediately below the plate, emitting fields driven by a 10 V power source and a pulsing circuit to generate 20 mT maximum-amplitude oscillating fields over two sequential 5 min trains at 50 and 385 Hz, respectively (10 min total exposure), with a pulse duty-cycle rise time of approximately 10 ms. This low energy Lf-PMF pulse-train exposure was used for initial exposures of T98G and SHSY brain tumor cell lines with reference to original studies using A549 lung cancer cells. For all experiments, control cells plated under equivalent conditions were incubated in parallel time course to that of Lf-PMF-exposed cells, without magnet exposure, but under otherwise identical conditions.

## Plasma membrane integrity assays

Cellular membrane integrity to outward protease leak was assayed immediately after Lf-PMF exposures using a luciferase-based cytotoxicity assay (CytoTox Glo, Promega G9291, Madison, WI) according to the manufacturer's instructions for 96W plate applications. The assay measures protease release into the medium of plated cell monolayers, with cells typically seeded in 96W plates 48 h before Lf-PMF exposure (with additional cell medium and handling conditions as detailed in "cell culture and field-exposure preparations" section above) to allow for plate attachment and establishment of robust subconfluent cell monolayers. In some studies to examine whether the effects of a Lf-PMF exposure on leak is reversible, we checked the field effect (i.e., protease release) after allowing as little as 15 min recovery time in culture, with replacement of fresh medium immediately after the 5 min Lf-PMF exposure period, and with comparison to sham-treated cells (i.e., transport of plate to magnetic platform area, but no magnetic exposure) treated otherwise under identical conditions. In this way, we assessed for continued protease release (i.e., irreversible/continuous cell stress) into a short recovery period over which protease leak into fresh medium could be detected with comparison to control.

As an additional proof-of-concept test of the induction of inward leak by Lf-PMFs, model A549 cells were grown on 96W cell culture plates to near confluency in 100 μL growth medium. Propidium iodide (PI) was added to appropriate wells at 25 μM, and cells were exposed to low-frequency magnetic pulsing conditions as published previously (6) over a low-energy solenoid platform. PI-supplemented medium was removed after magnetic exposure and the wells were washed twice with phosphate-buffered saline (PBS). The wells were then filled with 100 μL of PBS added to each well before assaying PI signal on a fluorescent plate reader.

## Sialidase enzymatic digestion and validation studies

For studies in which Sia digestion from cell surface glycans was employed, cells were exposed to 5 mU/mL of AUS Sialidase (Roche; Indianapolis, IN) diluted in normal growth medium for 1 h at 37°C. (For magnetic field exposures post-sialidase treatment, plated cells were exposed to the magnetic field immediately after sialidase incubation.) Sialidase activity was validated by examining the binding of the biotinylated lectins MAL-II (Vector Laboratories B1265; Newark, CA) or SNA (Vector Laboratories B1305; Newark, CA) to cultured, freshly harvested tumor cells +/− treatment with AUS sialidase. The lectins were incubated with the cells for 1 h at 4°C. Streptavidin-phycoerythrin (BioLegend 405203; San Diego, CA) was added to the lectin-labeled cells with appropriate washings, and signal was assayed by flow cytometry.

## Heparinase enzymatic digestion and validation studies

To destroy HS glycosaminoglycan chains exhaustively on the cell surface, heparin lyase III (Hep'ase; a kind gift from Dr. J. Esko) was used for 1 h at 12.5 mU/mL at 37°C. Cells were washed with PBS, followed by addition of fresh medium before subsequent experimental exposures. Testing of fluorescent FGF-2 binding to the cell surface was carried out by incubating biotinylated FGF-2 for 30 min followed by washing and streptavidin-phycoerythrin labeling, and flow cytometry: this was carried out to assess cell surface HS ligand binding capacity (as in (32)), where labeled FGF-2 is used as a well-established cell surface HS probe (33), and measured as a reporter for binding by flow cytometry on cells treated with and without Hep'ase, to assess HS digestion efficacy.

## Cultured cell proliferation assays

Beginning at the time of magnet exposure (24 h after cell seeding at $1 \times 10^5$ cells per well into 12W plates), cell growth was measured through daily cell counts harvested from plates over a 3 day time period. On any given day, 0.5% trypsin 0.2% EDTA solution was used to harvest cells from plates, and cells were counted through use of an automated hemocytometer (Countess II, Life Technologies; Carlsbad, CA).

## Reactive oxygen species generation assays

A549 tumor cells were incubated with 10 mM $H_2$DCFDA reactive oxygen species (ROS)-sensitive fluor reagent (DCF; Invitrogen D399; Carlsbad,

CA) in PBS for 30 min at 37°C, similar to reagents and methodology in (34). All non-DCF cells were incubated in PBS for the same time period. Cells were returned to normal growth medium after treatment and incubated for 30 min at 37°C. A baseline reading was performed after incubation. Some cells were exposed at room temperature to the standard 5 min exposure to a MagVenture (centered at the high-intensity zone; 80 T/s, 70 $\mu$s pulse width) magnetic field while others (controls) rested unexposed on the same bench. Plates were then assayed for fluorescence at time 0, 30 min, 1 h, and 3 h post-exposure. (In an additional subset of cells, heparanase pretreatment before Lf-PMF exposure was used as an additional control to eliminate HS from the cell surface.) Fluorimeter (FITC-detection) measurements for the DCF signal were then made on a 96W plate-reader fluorimeter (Becton; Franklin Lakes, NJ), and data were averaged from multiple (6) replicate measures per condition. Fluorescence signal of cells in the same medium but otherwise unexposed to DCF at the same time points was used as the background signal for each time point.

### Statistics

For most experiments, means were compared using Student's *t*-test with *p* value for significance at a cutoff of 0.05. Paired *t*-tests were used where appropriate (e.g., comparing paired data for mean protease leak after Lf-PMF exposure versus mean for Lf-PMF exposure postenzyme treatment in paired-measurement experiments). For all experiments, mean (reported with $\pm$ SD) for multiple wells treated under unique conditions (e.g., no-magnet control versus Lf-PMF exposure) was used for statistical comparison. If multiple experiments were carried out with high variability in mean control values, data normalized to 1.0 (for control) were tested for mean stimulation values significantly above 1.0 in multiple experiments, with significance (for mean $\pm$ SD for *n* trials) reported using the one-sample *t*-test. In the rare case where multiple Lf-PMF exposure measurements relative to control were recorded on a different day with comparison to multiple Lf-PMF measurements after Hep'ase treatment relative to control measured on a different day, then the appropriate unpaired *t*-test was used (comparing means in two independent and unpaired data sets). Number of trials (*n*) for each set of experiments is indicated in figure legends, along with *p* values.

## RESULTS

### Exposure of brain tumor cells to distinct Lf-PMF platforms affects membrane protease leak

A variety of malignant brain neoplasms overexpress key anionic-charged glycans, including Sia on a variety of glycan termini as well as anionic glycosaminoglycan polymers on membrane proteoglycans, which may play roles in transducing EMFs driven by an external Lf-PMF source (6,18,22). To examine how such transduction may affect tumor membrane integrity, we initially exposed 96W-plated T98G glioblastoma and SH-SY5Y neuroblastoma monolayers (named "SHSY" herein) at subconfluence to a low-intensity Lf-PMF solenoid platform delivering a 20 mT maximum field (dB/dt $\sim$ 2 T/s) with pulses over a 10 ms duty cycle at 50 Hz (as originally employed in (6)). After a 5 min exposure at room temperature, cells were immediately assayed for protease leak using a commercial luciferase-based assay. While a very modest but significant leak was detected immediately after Lf-PMF exposure compared with that of parallel control nonexposed cells (Fig. 1 *A*), exposure over the same period to a high dB/dt system (MagVenture coil, driving Lf-PMF 80 T/s pulse trains across plated cells over a 70 $\mu$s duty cycle at 15 Hz) resulted in markedly increased leak in both T98G and SHSY cells, as demonstrated in individual representative experiments (Fig. 1 *B*) as well as the means of multiple trials (Fig. 1 *D*). In this high dB/dt system, we placed plated cells within a pulsing magnetic field running perpendicular through 96W-plated cell monolayers, and protease leak appeared to be accordingly greater than that for cells placed over the much lower dB/dt solenoid platform (compare with Fig. 1 *A*).

### Common response patterns by a variety of malignant cells exposed to high-performance Lf-PMFs

Using a high-intensity MagVenture coil (as in Fig. 1 *C*), we demonstrate robust sensitivity of several tumor cell lines; including three malignant brain tumor lines, A172 glioblastoma, T98G glioblastoma, SHSY neuroblastoma, and a model lung carcinoma cell line A549 (originally used in low-intensity solenoid platform, as in (6)) exposed to two field intensities pulsing with magnetic flux perpendicular to the plated cells: 1) high dB/dt magnetic pulsing, with plated cells in a 96W cluster immediately within the highest intensity zone of the MagVenture trough-shaped coil system (dB/dt $\sim$ 80 T/s) and 2) lower dB/dt ($\sim$1.8 T/s) through cells clustered on a plate position a few cm distal to the highest intensity zone (see photographs in Fig. S1). Accordingly, as hypothesized, we demonstrated a significant fall-off in Lf-PMF-induced protease leak with distance from the trough center; and with the fall-off in T/s flux strengths with distance predicted from published (MagVenture, Cool-40 Rat Coil) (31) field-strength maps from which we could estimate dB/dt magnitudes for 96W cell clusters positioned near (dB/dt intensity of 80 T/s) and far (dB/dt intensity of 1.8 T/s) from the magnetic coil source (Fig. 2, tumor cell line data). Curiously, testing of nonmalignant cells for reference, we noted that exposure of primary mouse dendritic immune cells (as nontumor host cells of interest in a tumor microenvironment) to Lf-PMF under the same conditions did not result in leak after exposure (Fig. 2, *right*). Thermal effects of magnetic pulsing could be a consideration in generating protease leak; however, we did not note significant differences in temperature on the surface of medium-filled wells as a result of Lf-PMF pulsing, comparing near-coil well bases exposed to Lf-PMF $\sim$80 T/s with distal field exposed wells ($\sim$1.8 T/s), and to nonexposed (control) wells during real-time experimental benchtop conditions (Fig. S2). We also considered whether there was any immediate (ir)reversibility of such pulsed-field effects on leak by examining one of the model historical tumor (A549) cells under stringent conditions, employing Lf-PMF exposure at the high-intensity (80 T/s) condition while checking for continued protease leak early (i.e., within 15 min) after a medium wash at the completion of the 5 min Lf-PMF exposure. Under these conditions, we could not detect any greater protease leak by

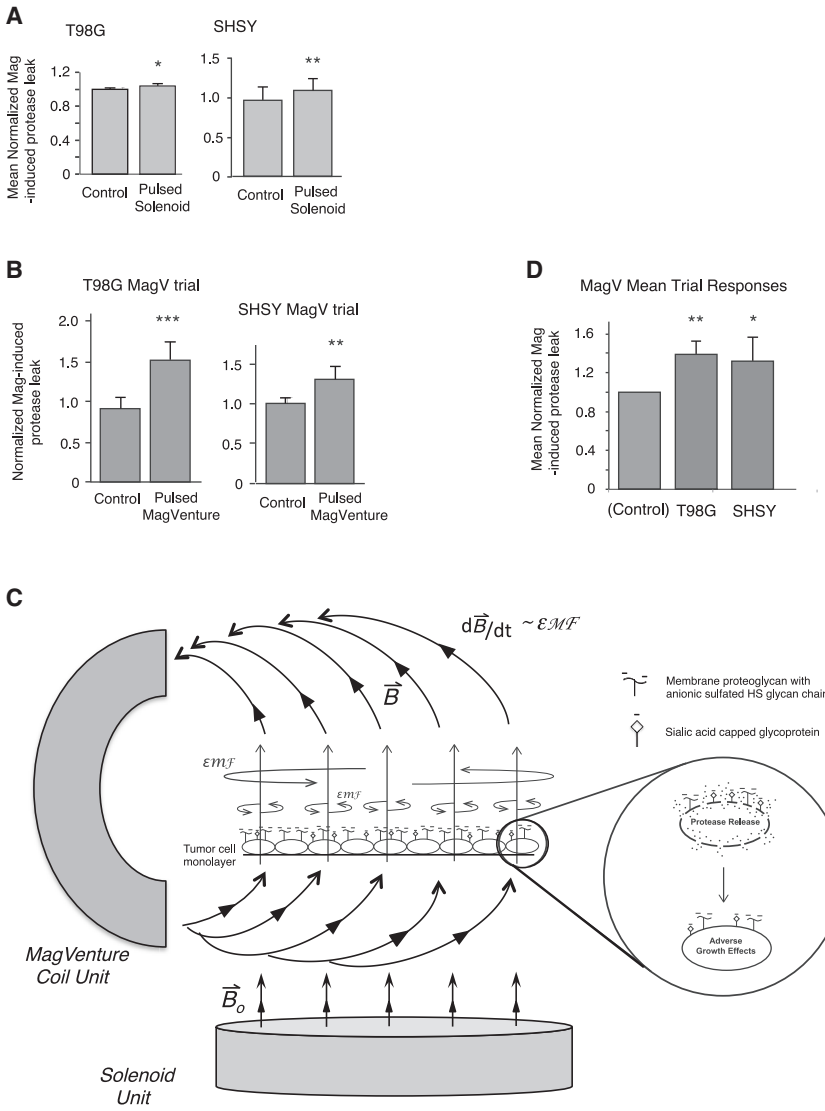


FIGURE 1 Effects of unique Lf-PMF exposures on membrane leak of brain tumor cells. (*A*) Monolayer plated cells of the Sia-overexpressing cell lines T98G (glioblastoma) and SHSY (neuroblastoma) plated at near-confluence were exposed to a very-low-intensity Lf-PMF solenoid system, delivering a 20 mT maximum field (dB/dt ∼ 2 T/s) over a 10 ms duty cycle at 50 Hz. After exposure, cells were immediately assayed for protease leak using a commercial luciferase-based assay that detects free proteases released into the medium. There was modest but significant leak detected after an exposure that included 5 min of this pulse train; $*p < 0.05$ (T98G cells) and $**p < 0.01$ (SHSY cells) for difference in means compared with control (normalized data from $n = 3$ separate experiments for each cell line). (*B*) Data from representative single-plate experiments for the same cell lines exposed to 5 min of a high dB/dt MagVenture system (driving Lf-PMF pulse trains with 80 T/s pulses over a 70 $\mu$s duty cycle at 15 Hz) is shown: normalized differences in mean responses relative to control are shown for T98G cells (*left graph*; for $n = 5$ control wells and $n = 9$ Lf-PMF exposed wells, $***p < 0.001$ for difference) and for SHSY cells (*right graph*; $n = 6$ control wells and $n = 9$ Lf-PMF exposed wells, $**p < 0.01$ for difference). (*C*) Illustrations of the MagVenture coil system used for cells as in (*B*), with a concept cartoon demonstrating a side view of plated cells within a pulsing magnetic field running perpendicular through cell layers on a 96W plate. The plate is placed at the edge of the trough-shaped coil on its side ("C"-shaped side view to the left; field strength shown as "B," and generated EMFs induced by dB/dt; with intensity falling off to the right with distance). For separate experiments of plated cells over a low-strength solenoid system, used for cells as in (*A*), instead of a high dB/dt MagVenture coil, the cylindrical solenoid underneath the plated cells generates low dB/dt EMFs wherein low-strength/longer duty-cycle B-field lines (*vertical arrows;* $B_o$) pulse from the solenoid core platform perpendicularly through plated cells. (*D*) Mean data from multiple experiments using the high dB/dt MagVenture system: differences in mean responses normalized to control are shown for T98G cells (*left bar*; for $n = 6$ independent experiments; $**p < 0.01$ for difference versus control) and SHSY cells (*right bar*; for $n = 5$ independent experiments; $*p = 0.055$ for difference).

Lf-PMF-exposed cells compared with basal protease leak by control (unexposed) cells over the same immediate recovery period. Examining for irreversibility at lower intensities was thus moot; and we present the graphed post-Lf-PMF recovery-period protease leak normalized to control in Fig. S3, showing no unique effect of Lf-PMF exposure on protease leak during the early recovery period. This suggests that any immediate post-Lf-PMF membrane leak under these conditions was reversible. Downstream tumor cell effects, however, may be another matter.

## Impact of Sia elimination from the brain tumor glycocalyx on Lf-PMF leak

A variety of brain tumor cell lines uniquely overexpress cell surface Sia, including the T98G glioblastoma and SHSY neuroblastoma cell lines; and even uniquely as polySia on the latter. Less is known about cell surface glycans and Sia overexpression on glioblastoma cells (or neuroblastoma cells) as a class. However, with examples in the literature (18,22,23) and knowing that the monosaccharide Sia, which is anionic at physiological pH, is frequently overexpressed in the glycocalyx of several tumors, including brain neoplasms, we asked whether Sia might possibly play a key role in transducing Lf-PMF-induced EMFs as a key electromechanical "coupling" component in the glycocalyx brain tumor cells. Strikingly, we found that the marked Lf-PMF-induced protease leak achieved by a short period of MagVenture pulses (i.e., 80 T/s dB/dt pulsed at 15 Hz, as shown in Fig. 1 *B*) could be abrogated by pretreating the monolayer-plated SHSY cells with AUS sialidase, which removes cell surface Sia immediately before Lf-PMF exposure (Fig. 3 *A*, *right bar*). More generally,

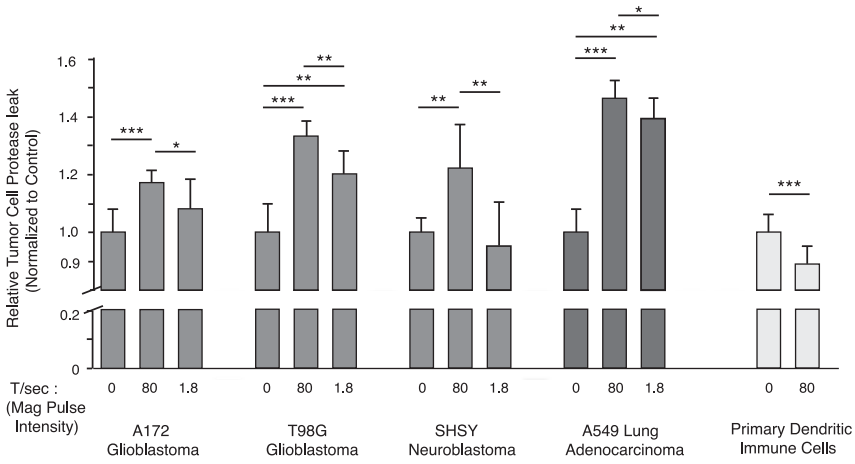


FIGURE 2 Effect of a high-performance Lf-PMF field on membrane leak in malignant cells and unique primary cells. Cells in monolayer 96-well dishes at ~80% confluence were treated for 5 min at room temperature to Lf-PMF exposures pulsed at 15 Hz using a MagVenture coil placed in lateral orientation, which allowed for exposure of cells to two magnetic field flux strengths by examining 9-well clusters in domains that are close (within 4 cm) or far (within 10 cm) from the edge of the pulsing source (i.e., trough coil oriented on its side). This allowed the Lf-PMF pulses with field lines running perpendicular to plated monolayers to expose near and far cells at two flux strengths: 1) 80 T/s or 2) 1.8 T/s (both using 15 Hz pulses delivered at duty cycle of 70 $\mu$s/pulse). Control cells were held at room temperature without Lf-PMF exposure for the same period. After the 5 min exposure period, cells were immediately assayed for protease leak using a commercial (Promega) luciferase-based assay that detects free proteases released into the culture medium. Cell leak was quantified normalized to that of control cells. Data represents mean of 9 wells for each magnetic flux strength per cell line, while respective controls were quantified from mean of 6 wells for most lines (3 wells for A549 cells). Far right: dendritic immune cells, as a primary cell line differentiated from bone marrow, were tested as a nontumor primary cell line. Significance for the differences in means between groups in graphs for tumor cells are indicated on the graph as $***p < 0.001$, $**p < 0.001$, $*p < 0.05$ for the indicated differences.

while multiple trials with results similar to that of Fig. 3 *A* demonstrated complete or near-complete abrogation of the high-intensity Lf-PMF-mediated leak in SHSY cells by pretreatment with AUS sialidase, trials using T98G cells demonstrated a lower (albeit still significant) effect of AUS pretreatment in inhibiting the Lf-PMF-driven leak. The data for multiple experiments in both tumor lines are summarized in Fig. 3 *B*, and suggests that glycocalyx Sia on T98G cells may play a lesser role in transducing pulsed EMF-mediated leak than that of SHSY cells (note near-complete abrogation of leak in SHSY cells pretreated with the enzyme [Fig. 3 *B*, *right bar*]). (As an additional control, baseline protease leak from AUS-treated cells not exposed to Lf-PMF was not significantly different from untreated control cells[Fig. S4].) We illustrate AUS-mediated digestion of Sia from the glycan termini of mucin glycoproteins overexpressed on tumor cells (Fig. 3 *C*, *cartoon*), releasing negatively charged Sia from the glycocalyx through AUS-mediated Sia hydrolysis. We also demonstrate the presence and marked reduction in surface Sia in AUS-treated SHSY cells by flow cytometry using fluorescent lectins (MAL-II and SNL) that bind to surface glycans expressing either α2,3-linked (MAL-II specific) or α2,6-linked (SNL specific) terminal Sia (35) on the surface of SHSY cells. Treatment with AUS markedly reduced binding of both lectins to SHSY cells (Fig. 3 *D*).

## A biophysical basis for induction forces on the tumor glycocalyx during magnetic pulsing

As a general model of anionic glycan components in the tumor glycocalyx with which EMFs driven by Lf-PMFs may interact, distinct tumor cells overexpress certain glycoproteins and proteoglycans with heavily expressed anionic/charged glycan components projecting into the glycocalyx. In a variety of brain tumor cells, Sia overexpressed on glycoproteins may "dominate" as an anionic glycan species in the tumor glycocalyx. Alternatively, sulfated anionic glycosaminoglycan chains of HS or chondroitin sulfate may be overexpressed by a variety of distinct tumors (e.g., HS on A549 lung carcinoma as an example), with anionic glycan chains that can transduce pulsed magnetic field-induced EMFs into molecular/glycocalyx force (and possibly motion). We conceptualize the latter in Fig. 4 *A*, wherein target molecules for magnet-induced EMF motion and resultant tumor cell membrane disruption consist of charged glycans that are overexpressed in a glycocalyx "canopy" above the plasma membrane of carcinoma cells. The application of oscillating magnetic fields (illustrated by vertical B-field lines in Fig. 4 *A*) with induced EMFs proportional to dB/dt (with pulse interval dt), allow for engagement of induced EMF/voltage paths orthogonal to the pulsed magnetic field lines with charged anionic tumor glycans in the glycocalyx. The induced EMF may impart torque (as illustrated in Fig. 4 *A*) about the base/attachments of core proteins to the membrane, associated membrane leak, and disruption in membrane integrity and tumor cell stress. The downstream induction of ROS as well as parallel antioxidant pathway induction has been described after the exposure of mammalian cells to pulsed magnetic fields under a variety of conditions (36). While control nonexposed model tumor cells appear to demonstrate a steady mild increase in ROS generation over a 3 h observation period of serial ROS measurements after sham exposure (i.e., plated control cells on the bench away from the magnetic field at room temperature for 5 min), magnet-exposed cells subjected to a standard narrow pulse-width MagVenture Lf-PMF pulse train (5 min, 80 T/s, 70 $\mu$s pulsing) show an early significant increase in ROS production at 30 min postexposure (i.e., significantly higher relative to baseline than that of control cells), while showing a relative "dip" in ROS

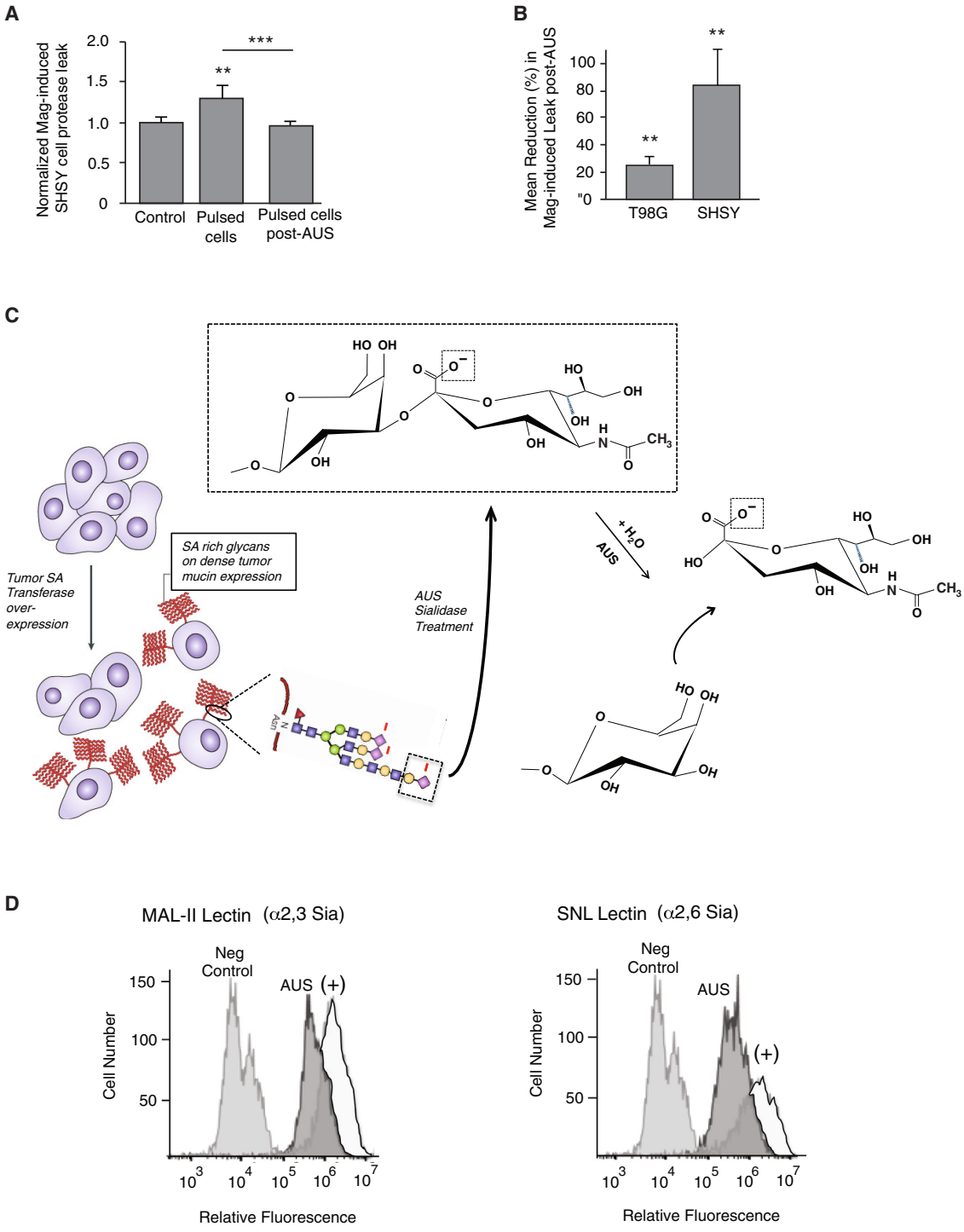


FIGURE 3 Impact of Sia in the glycocalyx on Lf-PMF leak: Effect of AUS sialidase Sia elimination. (*A*) Lf-PMF exposure (5 min MagVenture pulses at 80 T/s dB/dt using a 15 Hz train) results in protease leak (*middle bar*) normalized to baseline, while protease leak after treatment of SHSY cells with AUS sialidase (which removes cell surface Sia) was sufficient to abrogate the Lf-PMF-mediated leak (*right bar*); $^{**}p < 0.01$, $^{***}p < 0.001$ for difference in means, $n = 6$ wells for control and $n = 9$ wells for Lf-PMF exposure in each experiment (data representative of 4 independent experiments). (*B*) Mean reduction in Lf-PMF-induced membrane leak achieved by AUS sialidase pretreatment in T98G cells and SHSY tumor cells was assessed in multiple trials: graph shows mean inhibition in Lf-PMF leak as a result of AUS pretreatment; $^{**}p \leq 0.01$ for mean inhibition relative to non-AUS Lf-PMF-exposed cells; mean of $n = 3$ experiments for T98G cell line and $n = 4$ experiments for SHSY cell line. (*C*) Illustration of AUS sialidase elimination of anionic tumor surface Sia (noted as "SA" in figure text) on complex branched glycans decorating tumor glycoproteins. AUS digests α2,3- or α2,6-glycosidic linkages that link terminal Sia (*pink diamond*) to galactose residues (*yellow circle*) on heavily branched terminal glycans on the cancer cell surface (*zoom inset*), overexpressed on tumor glycoproteins (including mucins). (*D*) To assess the presence and reduction in surface Sia in AUS-treated SHSY cells, flow cytometry was carried out using

*(legend continued on next page)*

generation at the 1 h postexposure point (Fig. S5), after which they show a similar ultimate increase in signal (relative to baseline) as that seen in control cells at 3 h poststimulation. This "fluctuation" compared with controls is noted with time point comparisons in serial ROS measurements in Fig. S5. Eliminating HS from the tumor cell surface immediately before the exposure did not significantly change the temporal ROS profile after Lf-PMF exposure under these conditions (data not shown).

To also confirm Lf-PMF-induced leak through an alternate method, we assessed inward leak of an exogenous standard indicator (PI) during exposure of model A549 tumor cells to low-frequency magnetic pulsing conditions using a well-established solenoid field to reference results to that of protease leak (as an outward Lf-PMF-induced leak) under conditions identical to those we previously published using the same tumor cells (6). Interestingly, inward leak of exogenous PI into tumor cells immediately after the short Lf-PMF exposure was significantly greater than that of control cells unexposed to the magnetic field, but otherwise under identical conditions (Fig. 4 *B*). The degree of leak in Lf-PMF-exposed tumor cells over that of control during the exposure period compared reasonably with the magnitude noted for outward leak of protease using our CytoTox assay system in the same cells under the same exposure conditions (comparing protease and PI bars in Fig. 4 *B*).

## Distinct glycan species serve as major EMF transducers in distinct tumor-glycocalyx systems

In a series of ($n = 4$) independent trials paired with AUS testing wherein we employed a mean dB/dt $\sim$ 80 T/s in SHSY cells, and where the mean protease leak is nearly 40% over background in a 5 min period of Lf-PMF exposure (Fig. 5 *A*, *graph*, *middle bar*), exhaustive digestion of cultured cells with AUS is sufficient to achieve near-complete abrogation of cellular Lf-PMF-induced leak after enzyme treatment (i.e., to under 10% over background; Fig. 5 *A*, *graph*, *right bar*). Conceptually, this is consistent with glycocalyx dominated by Sia modifications (Fig. 5 *A*, *illustration, right*) as the major anionic species, and where susceptibility to Lf-PMF-induced EMFs falls markedly after digesting Sia as a "dominant" glycan in the system that may be largely responsible for the ability of SHSY glycocalyx to mediate electromechanical transduction. From another standpoint on the quantitative importance of Sia on magnetosensitivity, while one could quest to experimentally boost Sia expression and thus magnetosensitivity by feeding tumor cells increased Sia in the medium as a proof-of-concept, cells bearing high cell surface Sia expression (e.g., tumor cells herein) appear to be resistant to such attempts as shown in metabolic labeling studies (37). Nevertheless, by another rationale comparing Sia surface expression in distinct tumor-specific cell lines, it is noteworthy to consider Sia expression in the glioblastoma cell lines A172 and T98G, which show distinct magnetosensitivity when exposed to identical Lf-PMF pulsing conditions. In particular, we note that Lf-PMF exposures, as demonstrated in Fig. 2, result in greater impairment in membrane integrity in T98G cells compared with A172 cells. Accordingly, using flow cytometry (Fig. S6) to examine MAL-II lectin binding (which binds to a predominant motif of terminal $\alpha$2,3-linked Sia or alternatively to a non-Sia-sulfated galactose motif (38)), we demonstrate both a greater lectin affinity for T98G cells (>40% increase in mean fluorescence) compared with A172 cells, and a markedly greater reduction in binding after AUS sialidase treatment of T98G cells (92% reduction) compared with A172 cells (64% reduction). This greater sialidase sensitivity (Fig. S6, *right histogram*) suggests a markedly higher Sia presence on the T98G cell surface, and the correlation with magnetosensitivity is noteworthy in this light.

On A549 lung adenocarcinoma cells, surface HS appears to be the critical glycan that may be involved in transducing membrane leak in response to Lf-PMFs. We know from previous work that HS glycosaminoglycans may play a critical role as mediators of a Lf-PMF effect in this context, as the Lf-PMF effect is completely abrogated in A549 cells pretreated with exhaustive heparinase-mediated clearance of cell surface HS before the MagVenture 80 T/s Lf-PMF stimulus (Fig. 5 *B*, *graph*, and *cartoon to right*). Interestingly, while HS glycosaminoglycans may thus serve as a "dominant" EMF-sensitive glycan in the A549 glycocalyx, we had noted in separate studies that pretreatment of A549 cells with AUS sialidase before the Lf-PMF exposure was sufficient to inhibit Lf-PMF-induced protease leak by approximately 70% (albeit incompletely; Fig. S7), suggesting a complementary effect of Sia in mediating Lf-PMF effects on the "HS-dominant" tumor glycocalyx of A549 cells.

On the subject of HS as a dominant glycan in A549 glycocalyx, and the distinct compositions of glycocalyces in A549 versus SHSY cells, it is notable that, upon testing for HS presence (and sensitivity to digestion) on the surface of these tumor cells, very unique patterns are found. In particular, using a fluorescent FGF-2 probe for HS on the cell surface, while A549 cells are characterized by marked shifts in the mean fluorescence intensity for FGF-2 binding (as well as reduction upon heparinase digestion), SHSY cells show markedly lower shifts (Fig. 5 *C*), indicating likely greater levels of HS in the glycocalyx of A549 cells

fluorescent lectins (MAL-II and SNL) to bind with terminal Sia-expressing glycans on the surface of SHSY cells. Right graph shows marked SNL binding (depends on cell surface $\alpha$2,6-linked Sia), comparing far-right SNL (+) control with negative control at the left. AUS reduced SNL binding by $\sim$70% (leftward shift in "AUS" curve on log scale). MAL-II binding (depends on $\alpha$2,3-linked Sia) was >60% reduced (*left graph*); noting leftward shift in "AUS" curve relative to (+) control. To see this figure in color, go online.

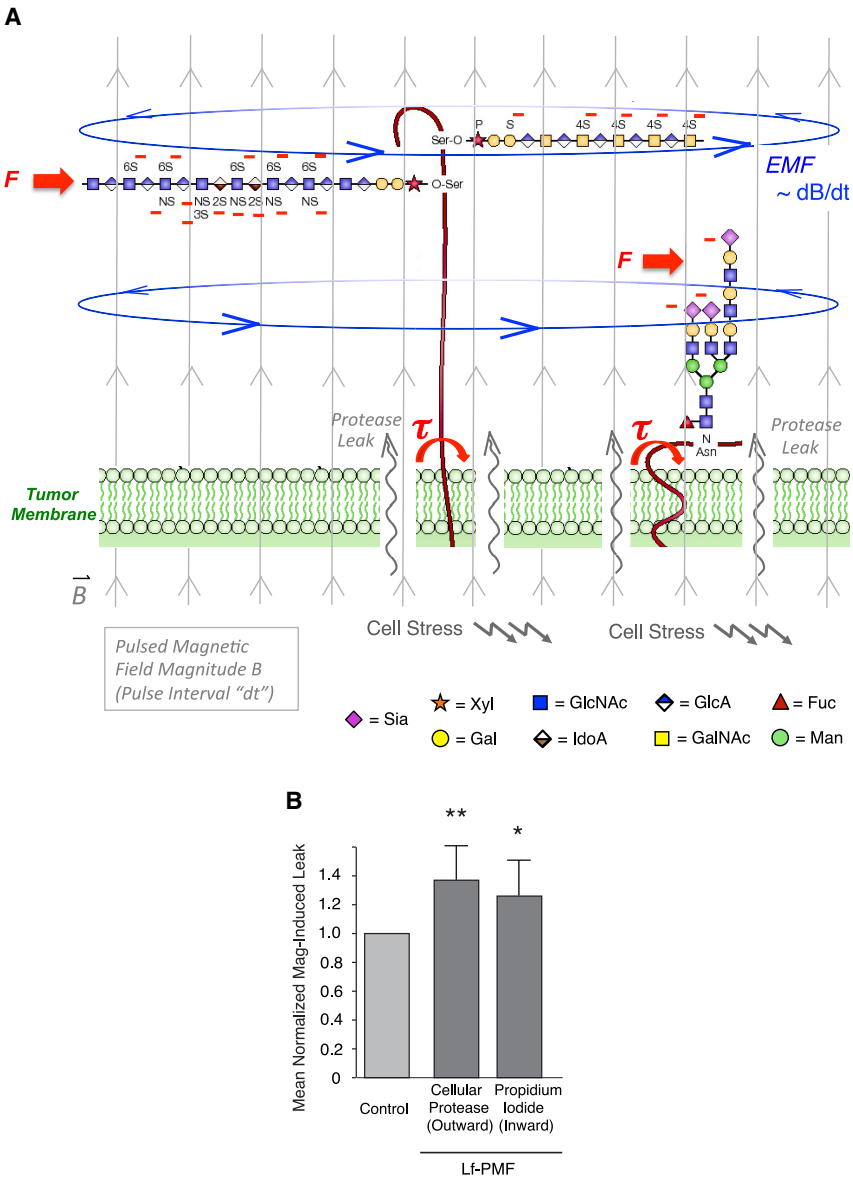


FIGURE 4 Concept and biophysical basis for induction forces on the cancer glycocalyx during magnetic field pulsing. (*A*) Target molecules for magnet-induced EMF motion and resultant tumor cell membrane disruption are charged glycans overexpressed in a glycocalyx "canopy" above the plasma membrane of carcinoma cells. These include: 1) proteoglycans (*left*), composed of anionic sulfated glycosaminoglycans such as heparan sulfate (HS) and chondroitin sulfate (CS) attached to core proteins. HS and CS chains are shown O-linked via xylose to the core protein, modified by anionic N-sulfation and 2S, 6S, and/or 3S sulfation (on HS) or 4S sulfation (on CS). Anionic charge (*red dashes*) on heavily sulfated glycan domains overexpressed on the plasma membrane of several cancer subtypes mediates HS binding to basic amino acids on chemokines, tumor growth factors, and receptors. 2) Cell surface Sia residues that "cap" branched terminal glycans on carcinoma membrane proteins (*right*), typically expressed of O-linked mucin glycoproteins. They are also highly expressed on malignant membrane polySia (e.g., on small cell lung cancer and brain tumor cells). Application of external oscillating magnetic fields (vertical field lines; magnitude B) is shown, along with induced EMFs proportional to dB/dt, where dt is the pulse interval. Induced EMF/voltage in the diagram is shown as potential conduction paths (*blue*) orthogonal to pulsed magnetic field lines, engaging with charged/anionic tumor glycans in the glycocalyx, imparting force F (*red arrows*) on core proteins, and creating torque (tau symbol) about points anchoring core proteins to the membrane (*red curved arrows*). This may induce leak (*wavy gray lines*) of small molecules such as proteases and tumor cell stress. Glycan legend: Xyl, xylose; Gal, galactose; GlcNAc, *N*-acetylglucosamine; IdoA, iduronic acid; GlcA, glucuronic acid; GalNAc, *N*-acetylgalactosamine; Sia, sialic acid; Fuc, fucose; Man, mannose. (*B*) To measure membrane leak using an alternate method, examining inward leak of an exogenous standard indicator (propidium iodide. [PI]), standard Lf-PMF exposure of model A549 tumor cells to the solenoid field platform in the presence of exogenous PI indicated significant inward leak (*right bar*, normalized to control cells; $n = 6$ trials, $^{*}p = 0.05$ for difference versus control). This was comparable with the magnitude noted for outward leak of protease (using CytoTox assay system) in the same cells under the same exposure conditions (*middle bar*, normalized to control; $n = 6$ trials, $^{**}p < 0.01$ for difference versus control). To see this figure in color, go online.

compared with that of SHSY cells (consistent with quantitative findings by others (39)).

## DISCUSSION

Low-frequency oscillating magnetic fields have been applied to tumor cells in culture as well as in vivo tumor models, with striking inhibition of tumor growth in some platforms (see (3,4,9,11) as examples). However, mechanisms remain undefined and speculative for the most part. This is a barrier to translation and biological control. Unique properties of magnetically induced or direct electric fields, capable of either imparting EMF on charge (q) in the targeted space, include pulse frequency, pulse width (duty cycle), and maximum driving magnetic (B-field) magnitude. For electromagnetic waves employed directly as E-fields, frequencies capable of altering tumor membranes (demonstrated in the kHz range (40)) or as tumor-treating fields (41) and directional amplitude (i.e., Poynting vector) may be critical variables. However, electric fields are greatly attenuated at relatively short tissue depths. With this in mind and a vision to perturb deeply seated tumor cells without ionizing radiation, we manipulated pulsed B-fields in benchtop cell-based mechanistic studies, recalling the deep tissue-penetrating inductive power of pulsed magnetic fields. With either modality, critical variables that best "tune" a physical coupling with tumor cellular structures

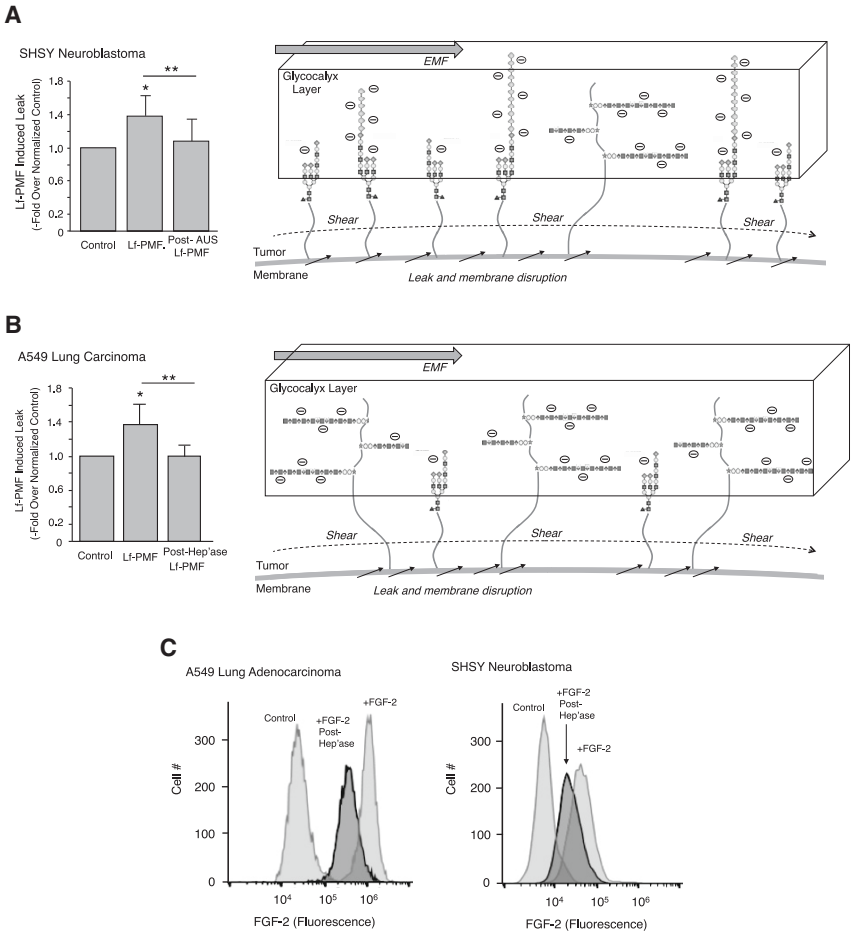


FIGURE 5 Lf-PMF-mediated leak and key roles for major EMF-transducing anionic glycocalyx component glycans. (*A*) Lf-PMF exposures (5 min MagVenture pulses at 80 T/s dB/dt using a 15 Hz train) were carried out in 96-well plates (as in Fig. 1 *B*) using SHSY neuroblastoma cells, resulting in significant protease leak over that of control cells (*graph*, *middle bar*; mean of $n = 4$ experiments; normalized to nonexposed control cells; $*p < 0.056$ for mean relative to control), while Lf-PMF exposure after treatment of SHSY cells with AUS sialidase was sufficient to nearly abrogate the Lf-PMF-induced leak (*right bar*; $**p < 0.01$ for difference between mean and that of Lf-PMF exposure). To the right, the cartoon shows membrane proteins projecting charged glycans (anionic charge depicted by circled "–" signs) overexpressed by tumor cells into the glycocalyx, depicted as a rectangular "slab" above the tumor membrane, shown as a long floating box. The conceptual example depicts a predominance of glycoproteins with anionic Sia (*diamond*) terminal monosaccharide modifications, or polySia that modify glycoproteins surrounding a representative proteoglycan shown to the right of center with anionic sulfated glycosaminoglycan chains. This "Sia-dominant" model may represent the typical surface of a brain tumor cell. A hypothetical pulse-induced EMF (*top gray arrow*) is shown engaging with the anion-rich glycocalyx to impart mechanical rightward force on the slab, creating membrane shear stress (via torque on transmembrane attachments), solute leak at the base (*black arrows*), and downstream cell stress. (*B*) Lf-PMF exposures were carried out on A549 lung adenocarcinoma monolayers. A significant increase in Lf-PMF-induced leak over that of nonexposed control cells was noted, shown in graph (*middle bar*; mean of $n = 3$ experiments; normalized to baseline; $*p = 0.013$ for mean relative to control). Treatment of A549 cells with heparin lyase (Hep'ase) was sufficient to completely abrogate the Lf-PMF-mediated leak (*right bar*; $**p < 0.01$ for difference between mean and that of Lf-PMF exposure response). To the right, hypothetical scenario for A549 glycocalyx exposed to Lf-PMF, where proteoglycan membrane proteins project a dominance of anionic sulfated HS glycosaminoglycan polymers into the rectangular glycocalyx slab. Again shown is pulse-induced EMF (*gray arrow*) now engaging with glycosaminoglycan rich glycocalyx to impart a rightward force on the slab. (*C*) Flow cytometry analysis of fluorescent FGF-2 binding to A549 and SHSY tumor cells as a probe for cell surface HS glycosaminoglycans, and the effect of Hep'ase. For A549 cells (*left graph*), marked shift in FGF-2 binding is shown (*rightmost histogram*) relative to negative control (*far left*). Treatment of cells with Hep'ase shows reduction in FGF-2 binding (*middle histogram*, +FGF2 Post Hep'ase). For SHSY cells (*right graph*), a markedly lesser shift in FGF-2 binding is shown, with leftward shift in post-Hep'ase.

(e.g., membrane, cytoskeleton, nuclear chromatin) remain a mystery. Moreover, "receiver" characteristics of the cellular or tissue elements with which such physical stimuli couple or interact have also not been well described. Even with some descriptions of the effects on cell behavior, how physical stimuli might be transduced remains a mystery. Although viability effects are not the focus herein, we previously showed that exposure of lung cancer cell monolayers to an oscillating solenoid platform generating Lf-PMFs over a 10 min period was sufficient to induce a modest but significant inhibition of tumor cell monolayer growth over subsequent days in culture relative to that of unexposed cells (6). Moreover, the dB/dt intensity data herein (e.g., as in Fig. 2) support that, at least in the generally low (or ultralow) frequency range, as long as the duty cycle for the pulse is far under the period of the pulse train, the dominating variable that affects membrane stress and leak may be the narrow pulse width rather than the absolute frequency per se. It is thus worth stressing that in our studies showing augmented membrane leak in response to increased dB/dt intensity (which determines the amplitude of the induced EMF), so long as a relatively "sharp" pulse can take place within the pulsing period, the ultimate frequency may not be as relevant as a short rise time for the pulsed field, allowing for potentially substantial biological effects that may be "tunable" by adjusting pulse width or B-field amplitude (dB/dt determinants) at very low frequencies.

Our interest in understanding how Lf-PMF-induced EMFs might be transduced via unique properties of glycans in the glycocalyx of brain malignancies prompted us to test brain tumor cells that commonly overexpress charged complex carbohydrate elements that may theoretically transduce the EMFs. Tumor plasma membrane leak (as originally measured in (6)) might ensue as a result of molecular attachment of the rich anionic EMF-susceptible tumor glycocalyx to the tumor

membrane, with shear forces at points of membrane attachment (8,16,18). We here examined leak of cellular proteases induced by Lf-PMF exposures of T98G glioblastoma and SHSY neuroblastoma cells known to overexpress glycans richly modified by anionic Sia residues, and with a theoretically distinct composition to that of Lf-PMF-susceptible A549 lung carcinoma glycocalyces that appear to be heavily endowed with anionic sulfated glycosaminoglycan chains. The basic observations of Lf-PMF-induced leak among all three lines of cells with their unique responses in distinct platforms and sensitivity to glycan modifications herein may provide critical mechanistic insights regarding how tumor glycocalyx might electromechanically transduce EMFs to altered membrane integrity and leak for which downstream effects on tumor cell behavior and survival may follow. In that light, we noted that, while low-intensity solenoid exposure of both T98G and SHSY tumor cells to a short Lf-PMF period was sufficient to induce a low but significant level of membrane leak (Fig. 1 *A*), the same short exposure was sufficient to modestly inhibit tumor monolayer growth and viability when cultured cells were quantified for three subsequent days in culture after short 5 min Lf-PMF exposures (Fig. S8). Although the latter is not our focus herein, the tumor viability effects are consistent with previous findings, and intriguing as effects secondary to transduction event(s) we examine herein.

Induced EMFs by pulsed magnetic fields in these studies must be generating unique leak effects above those caused by thermal background energy (which could also lead to a basal amount of protease leak). We gain some insight on this by demonstrating a "dose" effect within an expected range from the coil source using the MagVenture unit. Thus, as seen in distinct tumor cell lines in Fig. 2, a significant drop-off in Lf-PMF-induced leak occurs at a distance from the coil over which the B-field magnitude (and thus dB/dt) decreases markedly, albeit still with significantly greater leak than control at that lower-magnitude distance from the coil. This implies that pulsed fields at both positions must induce effects over that of thermal background (control condition); however, estimating the exact amount of energy above the thermal background is difficult since glycocalyx forces and shear effects over multiple cells may likely be operative. Indeed, using a very narrow pulse width (i.e., "dt" in dB/dt with values under 100 $\mu$s) may be favorable, along with the ability to simultaneously recruit charge in the entire glycocalyx "slab" over multiple cells. The wider spatial area (i.e., multicellular contiguous glycocalyx) over which the bounding EMF may interact with the glycocalyx "slab" of charge and mass, along with the use of narrower pulse widths (greater dB/dt) employed in any Lf-PMF platform, may induce substantial shear stress on tumor plasma membranes (as illustrated in Figs. 4 *A* and 5, *A* and *B*). In macroscopic tumor systems, the dB/dt "driving" effects for EMFs across macroscopic tumor fields might thus be "tunable" to generate greater cell stress with adjustments in pulse width (thus dB/dt) without necessarily changing pulse frequency or B-field magnitude, although one should not expect to necessarily observe "linear" downstream biological effects.

It is compelling to try to estimate an order of magnitude at which induced energy or currents generated by Lf-PMF excitation might operate in tumor cell systems with reference to thermal background energy in the system. Our empiric demonstration of dose effects (as discussed above) and sensitivity of the induced membrane leak to glycan elimination implicates energy phenomena operating well above the thermal background experienced by resting sham (nonpulsed) control cells. While tempting to somehow estimate this using B-field driving variables in our system, it is very difficult to predict actual electromotive energies (in Joules) that impact the glycocalyx of single cells versus multiple cells as monolayers in the system. Moreover, we must take into account the unique energies achieved using B-fields at narrow (milli- or microsecond) pulse widths. Narrowing the pulse width may impart additional order(s) of magnitude to the induced EMFs and energies, according to Faraday's law under a classical model (EMF $\sim$ dB/dt). Indeed, the narrow pulse width may be a key to achieving "driving" energies at orders of magnitude above the thermal background, $k_BT$ (i.e., Boltzmann constant $\times$ T(Kelvin)) at low pulse frequencies while operating at low/moderate driving B-field (milli-Tesla) strengths.

Moreover, EMF magnitude depends on the B-field flux area. Thus, in addition to pulse width, the summation of EMFs across multiple flux areas would need to be considered to estimate induced EMF-dependent effects over an integral of theoretical rings of potential/conduction involving contiguous glycocalyx over multiple cell contacts in tumor cell monolayers. This is challenging to measure, where any one EMF across flux area A (estimated by A $\times$ dB/dt) induces forces on a given charged glycocalyx ring bounding area A to release tumor cell proteases by that specific ring of cells. For a charged glycocalyx across a cell monolayer, this can vary widely over the diameter of the entire well (on the order of several millimeters), making it difficult to estimate which "rings" contribute to the summed EMFs that drive net cell leak in the well. Conceptually, in real tumors this summation of EMFs may be favorable given the ability to simultaneously recruit charge over contiguous tumor cell glycocalyces, and thus achieve wide spatial tumor stress effects over a 3D tumor multicellular population. These considerations also give insight to aim in future studies to directly observe glycocalyx movement with each pulse possibly using advanced microscopy systems. This might facilitate estimates of the real energies involved in macroscopic electromechanical coupling in tumor multicellular systems.

More generally, while introducing brain tumor cell lines in the system, and with the above insights on the importance of Sia overexpression in the glycocalyx of a variety of brain tumors, we focused on how Lf-PMF protease leak responses can depend on B-field strength, spatial characteristics, and

manipulation of tumor glycocalyx Sia in the system. In addition to greater magnitude effects by a higher intensity (T/s) pulsing system (compare Fig. 1, *A* and *B*), and the effects of spatial variation in B-field strength (high and low dB/dt in Fig. 2), we find key mechanistic importance in noting that Lf-PMF effects are sensitive to Sia elimination. AUS sialidase is capable of digesting terminal Sia monosaccharides linked through any possible Sia glycosidic bond to terminal galactose (i.e., α2,3- or α2,6-linked Sia), or to Sia itself via α2,8-linked Sia-Sia linkages in polySia polymers. The latter are likely to play an important role in expressing regions of high Sia density in the glycocalyx of SHSY or other brain or lung tumor cells (e.g., neuroendocrine tumors such as small cell lung cancer), where long Sia polymers are attached to unique tumor overexpressed membrane proteins such as neural cell adhesion molecules (23). In this setting, Lf-PMF-induced molecular motion of membrane core proteins heavily "decorated" with anionic Sia (or polySia) projecting into the tumor glycocalyx may result in EMF-driven membrane shear stress and leak dependent on Sia overexpression. Indeed, Lf-PMF-mediated protease leak from T98G and SHSY cell lines was sensitive to AUS pretreatment of tumor cells immediately before the Lf-PMF stimulus, with significant post-AUS reductions in leak for both cell lines, and near-abrogation of leak in SHSY cells pretreated with the enzyme (Figs. 3, *A* and *B* and 5 *A*, *graphs*).

The tumor glycocalyx may be regarded as a glycan "canopy" above the tumor plasma membrane, with a particularly heavy composition of anionic glycans. The latter are anchored broadly to the membrane by overexpressed proteoglycan and/or mucin core proteins that project attached glycans (anionic glycosaminoglycan chains and/or Sia modifications, respectively) densely into the canopy. We may envision how pulsed EMFs can interact with any "dominant" anionic glycan(s) in the canopy as a whole, essentially as an interconnected "slab." The important and likely "dominant" role that sulfated glycosaminoglycans such as HS may play in transducing Lf-PMF pulses into membrane leak in A549 cells is supported by the fact that Lf-PMF-induced leak is completely abrogated by pretreating cells with heparinase (which destroys HS chains) before Lf-PMF exposure (Fig. 5 *B*). It is notable that pretreatment of A549 cells with AUS sialidase before Lf-PMF exposure was sufficient to inhibit Lf-PMF-induced protease leak by ∼70% (Fig. S7). While heparinase pretreatment of A549 cells completely abrogates Lf-PMF-mediated leak, this AUS-mediated inhibition is appreciable, and suggests that destroying even a nondominant anionic glycan (i.e., Sia) in a tumor glycocalyx "dominated" by sulfated glycosaminoglycan chains as the major anionic species (as in A549 cells) may significantly alter the EMF-mediated effect. The data imply that Sia-modified glycan species might interact in some important way with HS glycosaminoglycans in the glycocalyx to mediate Lf-PMF effects. In this way, while HS is absolutely required for any Lf-PMF leak effect, loss of Sia also markedly inhibits the phenomenon: a simple biophysical concept that may reconcile this is that glycan-modified membrane proteins (or lipids) do not respond independently to EMF forces, but rather the overexpressed glycans on such molecules contribute to a common anionic glycan "bulk" in the tumor glycocalyx (i.e., as part of a larger rigid structure). Thus, EMF-driven responses may depend in a synergistic way on lattice-like properties of both dominant HS and "interspersed" Sia in a common glycocalyx slab.

It is also possible that species such as glycolipids (often overexpressed in brain tumors, with a high density of terminal Sia residues), HA, a sulfateless glycosaminoglycan (GAG) polymer that is also anionic, or other species are involved, possibly through shared presence and interaction within the glycocalyx as a mechanical unit. Thus, other magnetosensitive glycocalyx constituents may indirectly interact with overexpressed Sia residues or GAGs in a "cooperative" way, and with electromechanical sensitivity to chemical digestion of glycan components in the implicated cell lines. It is especially important to consider Sia-overexpressing glycosphingolipids (GSLs) as key gangliosides on brain tumor cells, and how these glycolipid species may also project Sia modifications heavily into the tumor glycocalyx (42). Unique specific gangliosides, including subsets that are more heavily sialylated (e.g., GD3 and GD2), appear to be present in high quantities on T98G cells, as distinct from GD1a and GM2 species that predominate on SHSY cells (43,44); however, the latter is characterized by heavier polySia expression, with numerous Sia residues polymerized on neural cell adhesion molecule core proteins (23). The latter may lead to unique magnetosensitivity of SHSY cells. Along with GSL growth signaling in lipid rafts (45,46), the sphingolipid acyl chains of GSLs can partially span the membrane to facilitate transmembrane events in the absence of transmembrane proteins (45). It is thus plausible to consider whether Lf-PMF repeated pulsing might alter or disrupt transmembrane events such as tumor growth signaling through unique mechanotransduction. This could be explored in future work. Accordingly, the implications on shifting to apoptotic signaling upon Lf-PMF-induced ganglioside signaling complex disruption becomes a plausible consideration.

Mechanisms mediating Lf-PMF-induced protease leak in tumor cells will need further dedicated investigation. Possible mechanisms include A) "molecular torque," wherein transmission of EMF-induced force on glycosylated charged molecular termini in the tumor glycocalyx transduce torque about transmembrane points of core-protein attachment to the malignant plasma membrane via the core protein shafts serving as "lever arms." B) Wave-like "rippling" of the glycocalyx slab over the malignant plasma membrane, and possibly associated membrane shear from pulsed movement of the broadly attached slab as a unit. In some tumors, the latter may include HA, a polyanionic nonsulfated glycosaminoglycan, wherein HA binding to the CD44 receptor overexpressed on the tumor plasma

membrane (47) may create more "anchors" of the broad glycocalyx slab via "free-floating" HA in the glycocalyx mass as a whole, with further potential to contribute membrane stress (at points of CD44 membrane attachment) and leak upon Lf-PMF-driven EMF engagement with the anionic mass as a whole. C) Direct interactions with submembrane EMF-sensitive components, including cytoskeleton, not necessarily transduced via the glycocalyx. Intriguingly, beyond outward cellular protease leak, we also confirmed that inward leak of exogenously added PI during Lf-PMF exposure alternatively demonstrates the Lf-PMF-induced membrane leak under identical conditions. The magnitude of leak under the two methods in the proof-of-concept was similar (Fig. 4 *B*), implying that induction-driven plasma membrane disruption/leak (rather than another mechanism leading to protease release into the exogenous environment) was operating as a result of the mechanism proposed in Fig. 4 *A* involving EMF-induced forces on the tumor glycocalyx.

Perhaps independent of the magnitude of leak and potential mechanical stress in the immediate subplasma membrane region is the possibility of an entirely unique cytoplasmic induction of free radical and ROS that has been cited in a variety of postpulsed magnetic field experimental scenarios in distinct cell systems (36). We included an assessment of this under our Lf-PMF pulsing conditions (Fig. S5) using model A549 tumor cells as a cell line in which low-frequency PMFs or even pulsed electric fields have been examined for ROS behavior (36,48,49); noting a unique variation in ROS signal postexposure with a distinct early rise followed by modest reduction or "dip" in ROS signal after 30 min poststimulation in Lf-PMF exposed cells, after which the recovered cells paralleled control ROS conditions. This behavior at 30 to 60 min post-exposure appeared to be reproducible in repeated experiments (of which Fig. S5 is representative), and suggests the possibility of an initial ROS stimulation in Lf-PMF pulsed tumor cells that induces compensatory antioxidant systems that might dampen or inhibit ROS presence in the period between 30 min and 3 h post-exposure. This is consistent with literature using the same tumor cell type in low-frequency PMF platforms, where reductions in ROS relative to control are seen (36), in contrast to higher-frequency or distinct longer-exposure conditions or in distinct tumor cell types. Whether these differences are influenced by distinct glycocalyx composition or correlate with associated glycocalyx-dependent leak remains to be explored, but the correlation of a unique ROS profile with Lf-PMF exposure is intriguing. Interestingly, while exogenous heparin has been shown to inhibit ROS production in distinct inflammatory cell types (50), our studies examine native tumor cell surface HS (which is "tethered" to the membrane as a key glycocalyx component in A549 tumor cells). Eliminating cell surface HS by pretreating cells with heparinase before Lf-PMF exposure did not appear to change the ROS temporal profile after exposure (discussed in results above). So possibly the fairly modest changes in ROS production resulting from Lf-PMF pulsing under our reported conditions may function through additional mechanisms within the tumor cell that may be independent of glycocalyx-induced leak. Work to discover additional mechanism(s) is outside our scope herein, but literature suggests highly variable ROS behavior in PMF-driven tumor cells, a variety of possible mechanisms, and active homeostatic compensatory pathways as well (36,51). Although the findings in Fig. S5 do not show dramatic effects of Lf-PMF exposure on ROS levels, we cannot falsify a hypothesis that ROS production (with possibly reactive scavenger effects) is involved in mediating magnetic field effects. If the latter is the case, it is difficult to estimate to what degree the pulsed-field effects might result directly from ROS-mediated mechanisms. The magnetic field effects can include either membrane leak (which our testing platform suggests is probably immediate) or downstream growth effects (Fig. S8). ROS production may also be driven secondarily to magnetic field effects (e.g., after an immediate first step of membrane leak induced by EMF-driven glycan-molecular torque and membrane stress), with subsequent effects on cell growth. Possibly, observing altered magnetic field effects after exhaustive addition of ROS scavengers to the system during Lf-PMF pulsing may further implicate a key role played by ROS production in the observed effects (with some caution to any broader and/or toxic effects of excessively high scavengers themselves). While beyond the scope of the studies herein, this might also be a useful way in future work to implicate a contribution of ROS production to the magnetic field effects.

Mechanisms (A) and (B) considered above seem plausible in a variety of tumors given loss of leak effects immediately after highly specific digestion of cell surface/glycocalyx glycans from the data of multiple experiments demonstrated here (Figs. 3 *B* and 5, *A* and *B*). These potential mechanisms may disrupt the membrane at points of proteoglycan or Sia-rich glycoprotein attachment to the membrane (18,22,52). Such forces and motion may also impact other channels/gates for larger molecules to leak during pulsed EMF-driven glycocalyx motion. While the type of stress that this induces in cancer cells remains to be defined, some preliminary studies (that have not necessarily explored cell surface mechanisms) do report alterations in tumor cell viability and/or apoptosis (4,10,11), but the conditions predicting these effects are undefined. We should also consider the possibility that Lf-PMFs may engage with a heavy interstitial glycan landscape that comprises tumor extracellular matrix: assessing Lf-PMF effects on this matrix in the setting of whole in vivo preparations in future work may guide an understanding of secondary effects in facilitating tumor immunological events (e.g., antitumor cytotoxic T cell access to tumor cell nests within tumor matrix), where we might also consider T cell penetration

induced by Lf-PMFs in some studies that examined tumor cell penetration by T cells after Lf-PMF exposures (9,53).

An entirely alternative model that can drive downstream biological effects from pulsed magnetic fields at relatively low energies would be a quantum spin model of radical pairs that may be operative. It involves magnetically induced changes in the spin of interacting electron pairs between singlet and triplet states that can drive reactions at otherwise energies even below the thermal background, and has been implicated in a variety of cellular biochemical reactions that impact biological processes (5). One interesting convention that may implicate the possibility of "active" magnetosensitive radical pairs in the system is the use of a second time-dependent magnetic field to modify or possibly even counter the effects of the original experimental field of interest (54). The second field must have frequency that matches one of the frequencies with which radical pair(s) oscillate between singlet and triplet states in the primary experimental (usually static) field. Identifying the range or key radical pairs for the latter might well be a challenge, and beyond the scope of this study, but it does allow us to consider other mechanisms that may result from unique Lf-PMF conditions in tumor cell systems. Moreover, if the system is "spin coupled," then one would expect there to be effects across those portions of the cells with atoms that have many electrons susceptible to spin-related effects (such as iron) and absent elsewhere. Interestingly, cancer cells exhibit greater dependence on iron compared with normal cells (55), and this could also be implicated in the differential effects.

Beyond carcinoma membrane biology and biophysics as well as the translational potential of incorporating such platforms into potential future tumor biomarker and therapeutic strategies, the transformative considerations of appropriately pulsed Lf-PMFs may be broad, opening a domain of biophysics that may harness pulsed magnetic fields to couple with unique membrane charge distributions in nature to selectively target the glycan surfaces of microbial pathogens or other biomolecules.

## CONCLUSION

Here, we present mechanistic support for a "first-physical" effect that Lf-PMFs may impart via EMF induction forces on the unique glycocalyx of tumor cells. This results in membrane protease leak, which is sensitive to specific elimination of anionic glycan species, such as Sia, as a dominant glycan in model brain tumor cells or sulfated glycosaminoglycans as dominant glycans on model lung carcinoma cells. This may represent a critical and "tunable" tumor-glycocalyx transduction mechanism via specific glycans depending on the malignant cell type, and provides further mechanistic understanding of Lf-PMF-driven tumor cell events that can lead to downstream tumor-directed cell stress in future translational strategies.

## SUPPORTING MATERIAL

Supporting material can be found online at https://doi.org/10.1016/j.bpj.2023.10.020.

## AUTHOR CONTRIBUTIONS

S.C.J. and P.G. performed most of the experiments, along with synthesis and analysis of preliminary data. Y.L. worked with S.C.J. on a subset of lung tumor cell studies. M.M.F. conceived and supervised all experiments, analyzed data interactively with the group, and guided preparation of key discussion, background, and figures. J.F. facilitated experimental apparatus utilization along with key discussion and insights during preparation.

## ACKNOWLEDGMENTS

We thank Dr. F. Furnari at UCSD for glioblastoma cell lines and Dr. D. Chen for SH-SY5Y neuroblastoma cells. We appreciate assistance by Dr. R. Rajasekaran for MagVenture unit support and assistance as well as Dr. J. Esko for heparin lyase III in addition to further thoughts and discussions. We are grateful for support from grants by the U.S. Department of Veterans Affairs (5-I01BX003688 to M.M.F.), the University of California San Diego Academic Senate (A149868 to M.M.F.), and the W.M. Keck Foundation (SERF-Friend; to J.F.) for funds in partial support of this work toward devising prototype magnetic field generators. M.M.F. is also supported by the Veterans Medical Research Foundation.

## DECLARATION OF INTERESTS

None to disclose.

## REFERENCES

1. Huang, M., P. Li, …, W. Li. 2022. Is Extremely Low Frequency Pulsed Electromagnetic Fields Applicable to Gliomas? A Literature Review of the Underlying Mechanisms and Application of Extremely Low Frequency Pulsed Electromagnetic Fields. Cancer medicine.
2. Kiełbik, A., W. Szlasa, …, J. Kulbacka. 2021. Effects of high-frequency nanosecond pulses on prostate cancer cells. *Sci. Rep.* 11, 15835.
3. Tatarov, I., A. Panda, …, L. J. DeTolla. 2011. Effect of magnetic fields on tumor growth and viability. *Comp. Med.* 61:339–345.
4. Tofani, S., D. Barone, …, F. Ronchetto. 2001. Static and ELF magnetic fields induce tumor growth inhibition and apoptosis. *Bioelectromagnetics.* 22:419–428.
5. Zadeh-Haghighi, H., and C. Simon. 2022. Magnetic field effects in biology from the perspective of the radical pair mechanism. *J. R. Soc. Interface.* 19, 20220325.
6. Ashdown, C. P., S. C. Johns, …, M. M. Fuster. 2020. Pulsed Low-Frequency Magnetic Fields Induce Tumor Membrane Disruption and Altered Cell Viability. *Biophys. J.* 118:1552–1563.
7. Gospodinov, A., and Z. Herceg. 2013. Chromatin structure in double strand break repair. *DNA Repair.* 12:800–810.
8. Hart, F. X. 2010. Cytoskeletal forces produced by extremely low-frequency electric fields acting on extracellular glycoproteins. *Bioelectromagnetics.* 31:77–84.
9. Nie, Y., Y. Chen, …, T. Wang. 2013. Low frequency magnetic fields enhance antitumor immune response against mouse H22 hepatocellular carcinoma. *PLoS One.* 8, e72411.
10. Koh, E. K., B. K. Ryu, …, K. S. Chae. 2008. A 60-Hz sinusoidal magnetic field induces apoptosis of prostate cancer cells through reactive oxygen species. *Int. J. Radiat. Biol.* 84:945–955.

11. Omote, Y., M. Hosokawa, …, H. Kobayashi. 1990. Treatment of experimental tumors with a combination of a pulsing magnetic field and an antitumor drug. *Jpn. J. Cancer Res.* 81:956–961.
12. de Seze, R., S. Tuffet, …, B. Veyret. 2000. Effects of 100 mT time varying magnetic fields on the growth of tumors in mice. *Bioelectromagnetics.* 21:107–111.
13. Zhang, X., H. Zhang, …, W. Xiong. 2002. Extremely low frequency (ELF) pulsed-gradient magnetic fields inhibit malignant tumour growth at different biological levels. *Cell Biol. Int.* 26:599–603.
14. Pall, M. L. 2022. Millimeter (MM) wave and microwave frequency radiation produce deeply penetrating effects: the biology and the physics. *Rev. Environ. Health.* 37:247–258.
15. Kang, H., Q. Wu, …, X. Deng. 2018. Cancer Cell Glycocalyx and Its Significance in Cancer Progression. *Int. J. Mol. Sci.* 19, 2484.
16. Fuster, M. M., and J. D. Esko. 2005. The sweet and sour of cancer: glycans as novel therapeutic targets. *Nat. Rev. Cancer.* 5:526–542.
17. Nagarajan, A., P. Malvi, and N. Wajapeyee. 2018. Heparan Sulfate and Heparan Sulfate Proteoglycans in Cancer Initiation and Progression. *Front. Endocrinol.* 9:483.
18. Pinho, S. S., and C. A. Reis. 2015. Glycosylation in cancer: mechanisms and clinical implications. *Nat. Rev. Cancer.* 15:540–555.
19. Rodrigues, E., and M. S. Macauley. 2018. Hypersialylation in Cancer: Modulation of Inflammation and Therapeutic Opportunities. *Cancers.* 10, 207.
20. Seidenfaden, R., A. Krauter, …, H. Hildebrandt. 2003. Polysialic acid directs tumor cell growth by controlling heterophilic neural cell adhesion molecule interactions. *Mol. Cell Biol.* 23:5908–5918.
21. Wade, A., A. E. Robinson, …, J. J. Phillips. 2013. Proteoglycans and their roles in brain cancer. *FEBS J.* 280:2399–2417.
22. Chin-Hun Kuo, J., J. G. Gandhi, …, M. J. Paszek. 2018. Physical biology of the cancer cell glycocalyx. *Nat. Phys.* 14:658–669.
23. Valentiner, U., M. Mühlenhoff, …, U. Schumacher. 2011. Expression of the neural cell adhesion molecule and polysialic acid in human neuroblastoma cell lines. *Int. J. Oncol.* 39:417–424.
24. Falconer, R. A., R. J. Errington, …, L. H. Patterson. 2012. Polysialyltransferase: a new target in metastatic cancer. *Curr. Cancer Drug Targets.* 12:925–939.
25. Amoureux, M. C., B. Coulibaly, …, D. Figarella-Branger. 2010. Polysialic acid neural cell adhesion molecule (PSA-NCAM) is an adverse prognosis factor in glioblastoma, and regulates olig2 expression in glioma cell lines. *BMC Cancer.* 10:91.
26. Wielgat, P., K. Niemirowicz-Laskowska, …, H. Car. 2021. Sialic Acid-Modified Nanoparticles-New Approaches in the Glioma Management-Perspective Review. *Int. J. Mol. Sci.* 22, 7494.
27. Cuello, H. A., G. M. Ferreira, …, M. R. Gabri. 2020. Terminally sialylated and fucosylated complex N-glycans are involved in the malignant behavior of high-grade glioma. *Oncotarget.* 11:4822–4835.
28. Bartik, P., A. Maglott, …, M. Dontenwill. 2008. Detection of a hypersialylated beta1 integrin endogenously expressed in the human astrocytoma cell line A172. *Int. J. Oncol.* 32:1021–1031.
29. Gupta, P., S. C. Johns, …, M. M. Fuster. 2020. Functional Cellular Anti-Tumor Mechanisms are Augmented by Genetic Proteoglycan Targeting. *Neoplasia.* 22:86–97.
30. Drakaki, M., C. Mathiesen, …, A. Thielscher. 2022. Database of 25 validated coil models for electric field simulations for TMS. *Brain Stimul.* 15:697–706.
31. Parthoens, J., J. Verhaeghe, …, S. Staelens. 2016. Performance Characterization of an Actively Cooled Repetitive Transcranial Magnetic Stimulation Coil for the Rat. *Neuromodulation.* 19:459–468.
32. Fuster, M. M., L. Wang, …, J. D. Esko. 2007. Genetic alteration of endothelial heparan sulfate selectively inhibits tumor angiogenesis. *J. Cell Biol.* 177:539–549.
33. Yayon, A., M. Klagsbrun, …, D. M. Ornitz. 1991. Cell surface, heparin-like molecules are required for binding of basic fibroblast growth factor to its high affinity receptor. *Cell.* 64:841–848.
34. Kim, H., and X. Xue. 2020. Detection of Total Reactive Oxygen Species in Adherent Cells by 2',7'-Dichlorodihydrofluorescein Diacetate Staining. *J. Vis. Exp.* 160
35. Zhang, X., H. Nie, …, X. L. Sun. 2018. Recent approaches for directly profiling cell surface sialoform. *Glycobiology.* 28:910–924.
36. Wang, H., and X. Zhang. 2017. Magnetic Fields and Reactive Oxygen Species. *Int. J. Mol. Sci.* 18, 2175.
37. Oetke, C., S. Hinderlich, …, O. T. Keppler. 2001. Evidence for efficient uptake and incorporation of sialic acid by eukaryotic cells. *Eur. J. Biochem.* 268:4553–4561.
38. Bojar, D., L. Meche, …, L. K. Mahal. 2022. A Useful Guide to Lectin Binding: Machine-Learning Directed Annotation of 57 Unique Lectin Specificities. *ACS Chem. Biol.* 17:2993–3012.
39. Yue, J., W. Jin, …, L. Wang. 2021. Heparan Sulfate Facilitates Spike Protein-Mediated SARS-CoV-2 Host Cell Invasion and Contributes to Increased Infection of SARS-CoV-2 G614 Mutant and in Lung Cancer. *Front. Mol. Biosci.* 8, 649575.
40. Chang, E., C. B. Patel, …, S. S. Gambhir. 2018. Tumor treating fields increases membrane permeability in glioblastoma cells. *Cell Death Dis.* 4:113.
41. Rominiyi, O., A. Vanderlinden, …, S. J. Collis. 2021. Tumour treating fields therapy for glioblastoma: current advances and future directions. *Br. J. Cancer.* 124:697–709.
42. Buffone, A., and V. M. Weaver. 2020. Don't sugarcoat it: How glycocalyx composition influences cancer progression. *J. Cell Biol.* 219, e201910070.
43. Sorokin, M., I. Kholodenko, …, R. Kholodenko. 2020. RNA Sequencing-Based Identification of Ganglioside GD2-Positive Cancer Phenotype. *Biomedicines.* 8, 142.
44. Dae, H. M., H. Y. Kwon, …, Y. C. Lee. 2009. Isolation and functional analysis of the human glioblastoma-specific promoter region of the human GD3 synthase (hST8Sia I) gene. *Acta Biochim. Biophys. Sin.* 41:237–245.
45. Head, B. P., H. H. Patel, and P. A. Insel. 2014. Interaction of membrane/lipid rafts with the cytoskeleton: impact on signaling and function: membrane/lipid rafts, mediators of cytoskeletal arrangement and cell signaling. *Biochim. Biophys. Acta.* 1838:532–545.
46. Sasaki, N., M. Toyoda, and T. Ishiwata. 2021. Gangliosides as Signaling Regulators in Cancer. *Int. J. Mol. Sci.* 22, 5076.
47. Mitchell, M. J., and M. R. King. 2014. Physical biology in cancer. 3. The role of cell glycocalyx in vascular transport of circulating tumor cells. *Am. J. Physiol. Cell Physiol.* 306:C89–C97.
48. Wang, S., Y. Hu, …, T. Liu. 2018. Sotetsuflavone inhibits proliferation and induces apoptosis of A549 cells through ROS-mediated mitochondrial-dependent pathway. *BMC Compl. Alternative Med.* 18:235.
49. Novickij, V., N. Rembiałkowska, …, J. Kulbacka. 2022. Pulsed electric fields with calcium ions stimulate oxidative alternations and lipid peroxidation in human non-small cell lung cancer. *Biochim. Biophys. Acta Biomembr.* 1864, 184055.
50. Dandona, P., T. Qutob, …, Y. Kumbkarni. 1999. Heparin inhibits reactive oxygen species generation by polymorphonuclear and mononuclear leucocytes. *Thromb. Res.* 96:437–443.
51. Reale, M., M. A. Kamal, …, N. H. Greig. 2014. Neuronal cellular responses to extremely low frequency electromagnetic field exposure: implications regarding oxidative stress and neurodegeneration. *PLoS One.* 9, e104973.
52. Sarrazin, S., W. C. Lamanna, and J. D. Esko. 2011. Heparan sulfate proteoglycans. *Cold Spring Harbor Perspect. Biol.* 3, a004952.
53. Nie, Y., L. Du, …, T. Wang. 2013. Effect of low frequency magnetic fields on melanoma: tumor inhibition and immune modulation. *BMC Cancer.* 13:582.
54. Hore, P. J., and H. Mouritsen. 2016. The Radical-Pair Mechanism of Magnetoreception. *Annu. Rev. Biophys.* 45:299–344.
55. Chen, Y., Z. Fan, …, C. Gu. 2019. Iron metabolism and its contribution to cancer (Review). *Int. J. Oncol.* 54:1143–1154.